Soliton Spectral Tunneling in Dispersion Controlled Holey Fibers

Francesco Poletti, *Member, IEEE*, Peter Horak, and David J. Richardson

***Abstract*—We design a number of index-guiding holey fibers with relatively simple structure which possess suitable dispersive properties for the observation of soliton spectral tunneling. Although the fabrication tolerances for these fibers are demanding, numerical simulations show that tunneling across a normal dispersion region of 150 nm width when pumped in the near infrared is in principle possible using just a few meters of these fibers.**

***Index Terms*— Nonlinear wave propagation, optical fiber devices, optical solitons.**

I. Introduction

The study of optical solitons and their propagation dynamics remains a hot topic since, as well of being of inherent fundamental physical interest, solitonic effects are key both to the generation of ultrashort pulses [1] and very broad supercontinuum spectra [2]. Classically speaking, optical solitons can only exist in the anomalous group velocity dispersion (GVD) regime, where dispersive broadening is balanced by nonlinear self-compression. As a result of intrapulse Raman scattering however, subpicosecond soliton pulses are also subject to a frequency downshift, an effect known as soliton self frequency shift (SSFS). Theoretical studies have shown that the SSFS can enable a soliton to tunnel through a spectrally-limited region of normal GVD [3]-[6]. Since this phenomenon shares many analogies with that of quantum mechanical tunneling through a potential barrier it is generally referred to as Soliton Spectral Tunneling (SST).

In order to experimentally observe SST, a fiber with a narrow normal GVD region surrounded by two regions of anomalous GVD is required. Such characteristics are difficult to achieve in conventional doped fibers but far less so in holey fibers (HFs) which provide access to a far wider range of dispersive properties due to the large refractive index contrast between glass and air. One possible HF design has recently been proposed for the observation of SST [6]. However, well in excess of 100 m of this fiber would be required to observe the effect, leading to acute issues in terms of fabrication tolerances. The scope of this Letter is to design more realistic HFs with suitable dispersion profiles for the observation of SST, and to understand the most critical issues both in the fabrication of these fibers and in the associated experimental realization of SST.

Manuscript received February 13, 2008;
This work was supported in part by the UK Engineering and Physical Sciences Research Council (EPSRC). The authors are with the Optoelectronics Research Centre, University of Southampton, SO17 1BJ, U.K. (e-mail: frap@orc.soton.ac.uk).

II. Inverse Fiber Design

We focus our attention on the simple silica HF structure shown in the inset of Fig. 1, which has 4 rings of air holes arranged on a triangular lattice with a pitch Λ. The diameter d_{out} of the two outer rings of holes is fixed to be 0.9 Λ in order to reduce the confinement loss to a negligible level, while the diameter d of the two innermost rings of holes is a free parameter to be optimized. Despite an improved confinement loss, the dispersive properties of these fibers are very similar to those of standard endlessly-single mode fibers with uniform hole size. Depending on the structural parameters d and Λ, the GVD profile can present either one zero dispersion wavelength (ZDW) or, more interestingly for this study, three ZDWs, $\lambda_1 < \lambda_2 < \lambda_3$. In this case, the normal GVD region is surrounded by two anomalous GVD regions and it is ideal for studying SST.

We systematically studied the fiber structure of Fig. 1 and found that it is possible to design HFs with arbitrarily closely spaced λ_1 and λ_2 at wavelengths shorter than the glass ZDW λ_G (~1300 nm for fused silica). The corresponding λ_3 however always lies far beyond λ_G, generating a normal dispersion region far exceeding the spectral width of any practical soliton. These fibers therefore are not suitable for SST applications [4], preventing the use of conventional fs sources around 800 nm and 1064 nm for the observation of these effects. As a result, in the following we will focus on pump wavelengths longer than λ_G, where HFs with an arbitrarily narrow normal GVD region between λ_2 and λ_3 can be obtained.

We calculate the fiber properties with a full vector finite element method (FEM) mode solver and optimize the structural parameters to provide suitable dispersive properties with an established inverse design technique [7]. We set the objective function, to be minimized with respect to d and Λ, as

$$V(d,\Lambda) = \alpha\left|D(\lambda_t) - D_t\right| + (1-\alpha)\left|DS(\lambda_t)\right| \quad (1)$$

where D and DS are the dispersion coefficient (in ps/nm/km) and the dispersion slope (in ps/nm^2/km), respectively, calculated at the desired wavelength λ_t. α is an empirical weight coefficient set to 0.01 to balance the magnitude of the two terms on the RHS of the equation, and D_t, the target value of the dispersion at λ_t, is set to -0.5 ps/nm/km, which generates a suitable separation between λ_2 and λ_3 of ~150-200 nm.

Table I shows the structural parameters of 7 optimized fibers, HF_1 to HF_7, corresponding to different values of λ_t. The corresponding dispersion curves are shown in Fig 1.

Note that fibers such as HF_1, where λ_t is too close to λ_G, can only support one ZDW, while as λ_t increases three ZDWs become possible ($\lambda_1 < \lambda_G$ is not visible in the Figure), the dispersion curves become steeper, and the width of the normal GVD region decreases. Note that the choice of a different D_t in (1) allows any arbitrary width of the normal dispersion region to be theoretically achieved with this HF design.

TABLE I
OPTIMIZED FIBERS

Fiber	(μm)	Λ (μm)	d/Λ	γ @ λ_i ($W^{-1}km^{-1}$)	Width of normal GVD region (nm)
HF_1	1.4	1.7352	0.32292	10.0	-
HF_2	1.5	1.7303	0.32873	8.8	258
HF_3	1.6	1.7308	0.33759	8.6	190
HF_4	1.8	1.7593	0.36392	6.6	159
HF_5	2.0	1.8143	0.39157	5.3	155
HF_6	2.2	1.8831	0.41857	4.8	149
HF_7	2.4	1.9570	0.44534	4.2	148

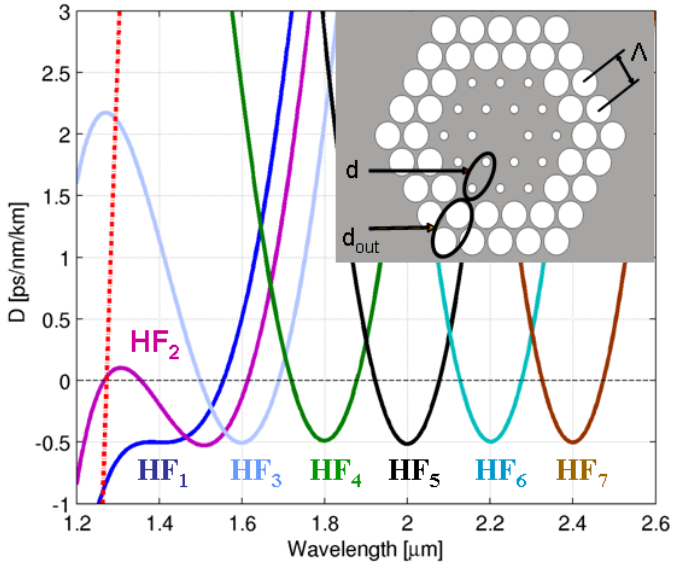

Fig. 1. Dispersion of 7 optimized HFs (the structure is shown in the inset).

III. NUMERICAL SIMULATIONS OF SST

To assess whether the fibers in Fig. 1 are suitable for SST, we implemented a program based on the classic symmetric split-step Fourier method with adaptive step size control, and solved numerically the generalized nonlinear Schrödinger equation (e.g. Eq. (2) in [2] with $\tau_{shock}=1/\omega_0$ and $\Gamma_R=0$). Our model includes the exact calculated dispersion curves shown in Fig. 1 and the frequency dependence of the loss, $\alpha(\omega)$, which we assume will be dominated by the intrinsic loss of the glass [8]. Fig. 2 shows the spectral evolution of a soliton undergoing SSFS–also referred to as a Raman or colored envelope soliton [4]–in a selection of fibers from Fig. 1. The pulse has a 50 fs FWHM, it is launched at a wavelength shorter than λ_2 and propagated for 30-50 soliton lengths. The results for HF_2 are not shown since due to the excessive width of the normal GVD region, we could not observe SST in that fiber, even if we increased the input pulse bandwidth by launching a pulse as short as 10 fs. Fig. 2(a) shows that HF_3 is also not suitable for SST of a 50 fs soliton, although it would work for 25 fs pulses (not shown). Fig. 2(b) shows that clean SST can be observed in HF_4; a similar result was found for HF_5 and HF_6 (not shown) and for HF_7 when fiber loss was neglected, Fig. 2(c). Fig. 2(d) however shows that if the loss (~4dB/m at the output wavelength of 2.6 μm) is included in the model, SST is suppressed, indicating that the multiphonon absorption edge of silica limits the longest useful wavelength to ~2.5 μm.

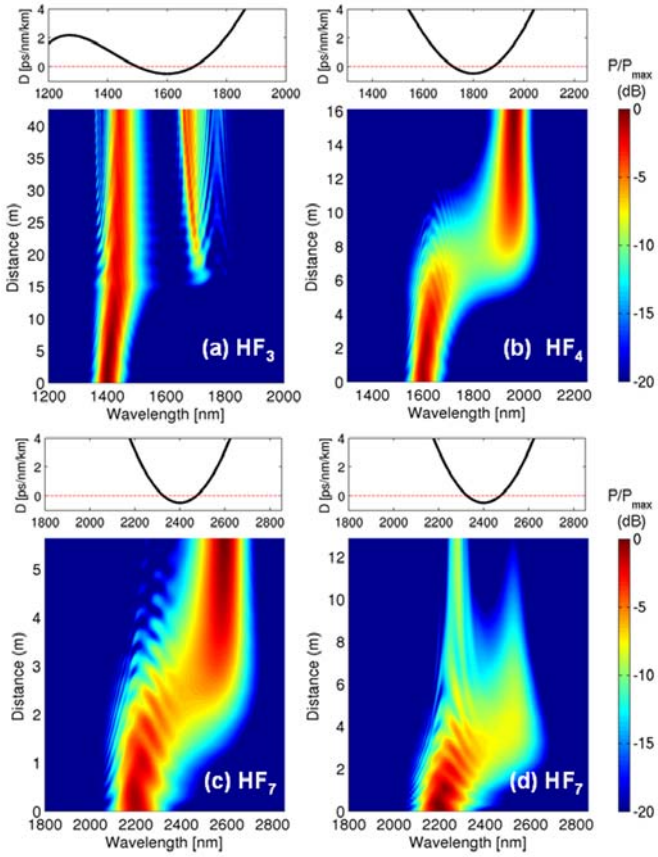

Fig. 2. Simulated logarithmic density plots representing the spectral evolution of a fundamental soliton as it propagates through (a) HF_3, (b) HF_4, (c) HF_7 when loss is neglected and (d) HF_7 with the inclusion of the glass loss.

It is also worth noting that since tunneling occurs normally within 10-20 soliton lengths, using a fiber with a steeper dispersion profile (i.e. larger $|\beta_2|$ at the input wavelength) is an effective way to reduce the required propagation distance, which is of the order of a few meters for our fibers, as opposed to ~350 m required for the fiber in [6]. Moreover, if the pulses are launched at shorter wavelengths, they will be moved towards wavelengths of lower GVD by SSFS and will thus be adiabatically compressed, which further reduces the required propagation distances.

IV. FABRICATION TOLERANCES

Having designed a number of structurally simple HFs suitable for the observation of SST, we investigated the sensitivity of the overall GVD to minor deviations from the optimum structural parameters. Fig. 3 shows the GVD dependence on d/Λ variations of the order of 1%. As can be seen, the curves shift to higher GVD values as d/Λ increases (similar results were obtained for Λ variations, although these are not shown here). It is also evident that fibers operating at a shorter wavelength are more tolerant to fabrication inaccuracy. However, as we showed in Fig. 2,

SST in fibers operating at shorter wavelengths require a longer propagation length and the benefits of the improved fabrication tolerance is offset by the need of a tight structural control over a longer length.

The results in Fig. 3 indicate that fabrication of a 5-15 m long fiber suitable for observing the SST would be challenging given the current ~1% fabrication dimension accuracies achievable –our results indicate that control of the structural parameters of the order of 0.1% will be necessary. Nevertheless the need to maintain this level of accuracy over relatively shorter length scales represents a significant improvement over previous fiber designs.

Finally, we illustrate a further issue associated with making a definitive experimental demonstration of SST. In Fig. 4 we plot the spectral evolution of a 50 fs soliton in the case of: (a) a fiber with 3 ZDWs and a suitable normal dispersion region (HF4); and (b) a fiber with fully anomalous dispersion obtained by up-shifting the dispersion profile of the optimum fiber as might be obtained by fabrication inaccuracy (see Fig. 3). In case (a) the pulse undergoes SSFS until a wavelength where a phase matching condition enabling tunneling is reached and an abrupt wavelength shift is obtained [5]. This is followed by a further period of SSFS. By contrast, in Fig. 4(b) the soliton is subject to SSFS along the whole fiber length and experiences an effective decreasing and subsequently increasing GVD due to higher order dispersion which results in the spectral behavior shown in the figure [3]. The output spectra, consisting of a red-shifted fundamental soliton and some residue of the input pulse, suppressed by 30 dB, look very similar in the two cases, highlighting the fact that some form of distributed measurement of the pulse evolution will be required for an unambiguous demonstration of SST.

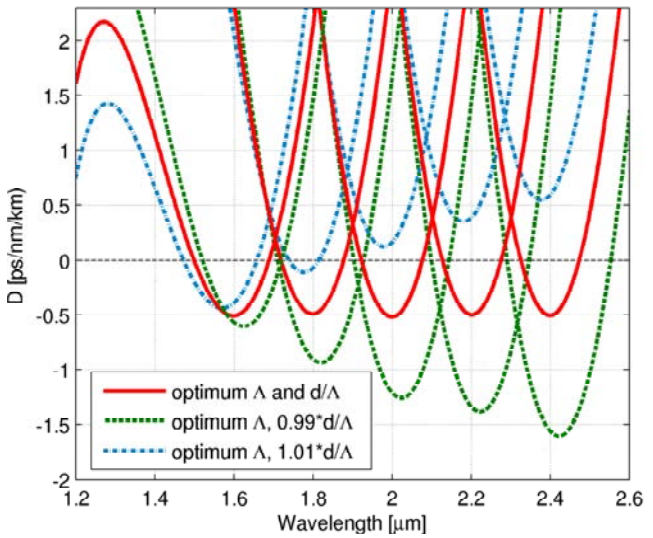

Fig. 3. Dispersion profile of the fibers in Fig. 1 resulting from variations of ±1% from the optimum d/Λ.

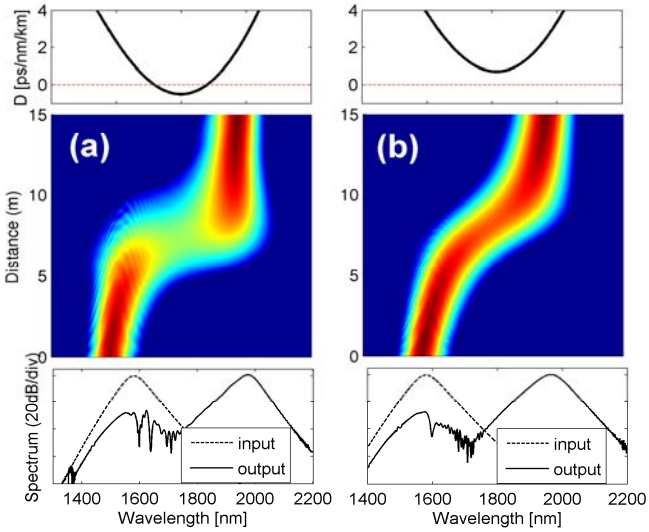

Fig. 4. Spectral evolution of a 50 fs soliton propagating in (a) HF_4, (b) a fiber, similar to HF_4, with optimum d/Λ and $1.01*\Lambda$.

V. Conclusion

We have designed realistic and simple silica-air HFs which are suitable for the experimental study of SST of sub-picosecond solitons. Production of these fibers would be challenging using current fabrication procedures, although the extremely short pulse durations now available [1] may relax the demanding fabrication tolerance somewhat, allowing SST to take place over wider regions of normal GVD. Future work could explore more complicated fiber designs that are even more fabrication-tolerant, while still allowing SST over short fiber lengths. Alternatively, non-silica glasses may provide higher nonlinearities and larger Raman frequency shifts. Finally, we stress the need for pulse evolution measurements to confirm any claimed experimental realization of SST.

Acknowledgment

The authors would like to thank J. Dudley and C. M. de Sterke for useful discussions on the SST phenomenon.

References

[1] M. A. Foster, A. C. Turner, M. Lipson, and A. L. Gaeta, "Nonlinear optics in photonic nanowires," Opt. Expr. vol. 16, pp. 1300-1320, 2008.

[2] J. M. Dudley, G. Genty and S. Coen, "Supercontinuum generation in photonic crystal fiber," Rev. Mod. Phys. vol. 78, pp. 1135-1184, 2006.

[3] V. N. Serkin, V. A. Vysloukh and J. R. Taylor, "Soliton spectral tunnelling effect," Electron. Lett. vol. 29, pp. 12-13, 1993.

[4] V. A. Vysloukh, V. N. Serkin, A. Yu, Danileiko and E. V. Samarina, "Influence of the dispersion-spectrum inhomogeneities on the Raman self-conversion of the frequency of femtosecond optical solitons", Quant. Electronics vol 25, pp. 1095-1100, 1995.

[5] E. N. Tsoy and C. M. de Sterke, "Theoretical analysis of the self-frequency shift near zero-dispersion points: Soliton spectral tunnelling," Phys. Rev. A vol. 76, 043804, 2007.

[6] B. Kibler, P. A. Lacourt, F. Courvoisier and J. M. Dudley , "Soliton spectral tunnelling in photonic crystal fibre with sub-wavelength core defect," Electron. Lett. vol. 43, pp. 967-968, 2007.

[7] F. Poletti, V. Finazzi, T. M. Monro, N. G. Broderick, V. Tse, D. J. Richardson, "Inverse design and fabrication tolerances of ultra-flattened dispersion holey fibers," Opt. Expr. vol. 13, pp. 3728-3736, 2005.

[8] O. Humbach, H. Fabian, U. Grzesik, U. Haken and W. Heitmann, "Analysis of OH absorption bands in synthetic silica," J. non-Cryst. Solids vol. 203, pp. 19-26, 1996.